Available online at www.sciencedirect.com
ScienceDirect
Journal of Catalysis 246 (2007) 74–90
JOURNAL OF CATALYSIS
www.elsevier.com/locate/jcat

Influence of CO_2 and H_2 on the low-temperature water–gas shift reaction on Au/CeO_2 catalysts in idealized and realistic reformate

Y. Denkwitz [a], A. Karpenko [a], V. Plzak [b], R. Leppelt [a], B. Schumacher [a], R.J. Behm [a,*]

[a] *Institute of Surface Chemistry and Catalysis, Ulm University, D-89069 Ulm, Germany*
[b] *Centre for Solar Energy and Hydrogen Research, Helmholtzstr. 8, D-89081 Ulm, Germany*

Received 18 September 2006; revised 7 November 2006; accepted 9 November 2006

Available online 22 December 2006

Abstract

The effect of CO_2 and H_2 on the activity and deactivation of Au/CeO_2 catalysts in the low-temperature water–gas shift reaction was investigated by combined kinetic and in situ IR spectroscopic measurements, going stepwise from idealized to realistic reaction atmospheres. The variation of the reaction atmosphere results in considerable variations in the initial activity and deactivation behavior, with significantly lower activity in the presence of H_2 and more pronounced deactivation in CO_2-rich gases. In situ DRIFTS measurements reveal a complex interaction of the different components in the formation of adsorbed reaction intermediates and side products. The bidentate formate species (1588 and 2833 cm^{-1}), which are dominant in H_2-free atmospheres and act as reaction intermediates, are replaced by less reactive bidentate (1560 and 2858 cm^{-1}) and bridge-bonded (2933 and 2961 cm^{-1}) formates in H_2-rich atmospheres. Deactivation is related mainly to the formation of thermally stable monodentate carbonates, which act as reaction-inhibiting spectator species. Their formation is enhanced by CO_2 in the reaction gas, whereas H_2 leads to their reactive removal by reaction to formates. Possible mechanisms for the deactivation process are discussed.

Keywords: Water–gas shift reaction; Realistic reformate; Kinetics; Gold catalyst; Au/CeO_2; CO_2; H_2; GC; DRIFTS

1. Introduction

Recently there has been renewed interest in the water–gas shift reaction because of its potential application in removing CO from CO-contaminated, H_2-rich feed gases for low-temperature polymer electrolyte fuel cells (PEFCs) obtained from, for example, the reforming of alcohols or fossil fuels [1,2]. Typical reformates contain 8–10% CO, around 20% CO_2, about 15–20% H_2O, and the balance mainly H_2. For PEFC applications, the CO content must be reduced to below 50–100 ppm to avoid poisoning of the anode catalyst [3]. This is commonly done by a combination of shift reactors (high-temperature shift (HTS; 300–400 °C), low-temperature shift (LTS; 200–260 °C)) [4] and selective CO oxidation (PROX), the latter of which removes the remaining CO to levels in the ppm regime. Currently, $Cu/ZnO/Al_2O_3$ is used as the standard LTS catalyst, but SiO_2-, MgO-, and Cr_2O_3-supported copper catalysts also have been applied [4]. Recent studies of the WGS reaction have shown also that supported gold catalysts, such as Au/ZrO_2, Au/TiO_2, and recently Au/CeO_2 [5], are surprisingly active catalysts for this reaction. However, most earlier studies were performed in idealized reaction gas mixtures, mainly in dilute water–gas (CO, H_2O, and N_2); the reaction in realistic reformate has been investigated only in a limited number of studies [6–8].

In this paper we report on the effect of CO_2 and H_2 and of more realistic, higher CO and H_2O concentrations on the activity and, in particular, the deactivation of Au/CeO_2 catalysts, going stepwise from an idealized reaction gas mixture (dilute water–gas) via addition of H_2 and CO_2 (H_2-rich idealized reformate, CO_2-containing idealized reformate, and H_2 + CO_2-rich idealized reformate) and increasing CO and H_2O content finally to realistic reformate (1/4 realistic reformate, 1/2 realistic reformate, realistic reformate, and H_2-free realistic reformate). These latter mixtures, which differ in terms of the total amounts of CO, CO_2, H_2, and H_2O but maintain a

* Corresponding author.
E-mail address: juergen.behm@uni-ulm.de (R.J. Behm).

0021-9517/$ – see front matter
doi:10.1016/j.jcat.2006.11.012

Table 1
Reaction rates over a 4.5 wt% Au/CeO_2 catalyst at 180 °C in different idealized and realistic reformate gas mixtures

Reaction gas mixture	Gas composition (kPa)	Catalyst dilution (mg catalyst + mg Al_2O_3)	Initial rate (mol g_{Au}^{-1} s^{-1})	Rate after 1000 min (mol g_{Au}^{-1} s^{-1})	Relative rate after 1000 min (%)
Idealized reformate	1 CO, 99 N_2 (dry); + 2 H_2O	6.8 + 68.3	4.5×10^{-4}	3.6×10^{-4}	79
H_2-rich idealized reformate	1 CO, 99 H_2 (dry); + 2 H_2O	48.1 + 47.2	2.2×10^{-5}	1.7×10^{-5}	77
CO_2-containing ideal. reformate	1 CO, 1 CO_2, 98 N_2 (dry); + 2 H_2O	7.0 + 70.0	3.0×10^{-4}	1.9×10^{-4}	63
H_2 + CO_2-rich idealized reformate	1 CO, 1 CO_2, 98 H_2 (dry); + 2 H_2O	90.8 + 0	2.3×10^{-5}	1.3×10^{-5}	56
1/4 realistic reformate	1 CO, 4.2 CO_2, 75.2 N_2, 19.6 H_2 (dry); + 5 H_2O	90.7 + 0	1.9×10^{-5}	8.8×10^{-6}	46
1/2 realistic reformate	2 CO, 8.4 CO_2, 50.5 N_2, 39.1 H_2 (dry); + 10 H_2O	91.9 + 0	5.9×10^{-5}	2.3×10^{-5}	38
H_2-free realistic reformate	4 CO, 16.8 CO_2, 79.2 N_2 (dry); + 20 H_2O	84.2 + 0	3.5×10^{-4}	1.3×10^{-4}	36
Realistic reformate	4 CO, 16.8 CO_2, 1 N_2, 78.2 H_2 (dry); + 20 H_2O	99.3 + 0	9.4×10^{-5}	2.8×10^{-5}	30

fixed CO:CO_2:H_2:H_2O ratio (see Table 1 for reaction gas mixtures), were included to stepwise proceed to the rather high CO, CO_2, and H_2O concentrations in realistic reformate. This work is part of a comprehensive study of the WGS reaction on these Au/CeO_2 catalysts. Recently reported results on the kinetics, the mechanism of the reaction, and the effects of catalyst loading for the reaction in idealized gas mixtures show that the reaction proceeds via formation and decomposition of surface formates, with decomposition of these formates being the rate-limiting step, and that it includes a dynamic equilibrium between formates adsorbed on the ceria support and formate species located on active sites for formate formation and decomposition [5]. The nature of these centers is not clear; possible candidates are sites at the perimeters of Au nanoparticles ("adlineation sites"), small Au clusters, or ionic $Au^{\delta+}$ sites. The pronounced decay of the Au-mass normalized activity with increasing Au loading for practically constant Au particle size (mean diameter ca. 2 nm) and ionic $Au^{\delta+}$ content (10%) was explained by contributions of CO adsorption on the ceria substrate within a given radius ("capture zone"), with subsequent reverse spillover to the Au nanoparticles and active sites.

Previous studies on the origin and mechanism of the deactivation of metal/ceria catalysts reached widely differing conclusions. On the one hand, several groups reported a more or less substantial deactivation of supported noble metal/ceria catalysts during the WGS reaction [6,7,9–12], which was attributed to overreduction of the support by H_2 [9], sintering of the noble metal particles [10,11], or partial blocking of the ceria support surface by surface carbonates and/or formates [6,12]. These reports are contrasted by a recent study of Andreeva et al. [13], who found no deactivation of Au/CeO_2 catalysts during the WGS reaction in idealized reformate at 140–350 °C over three weeks. But the widely differing results and reaction conditions in these studies do not provide a comprehensive understanding of the reaction process, particularly the roles of the individual components in realistic gas mixtures. The same is true for the deactivation behavior of these catalysts. These aspects are the topic of the present study.

In what follows, we will, after a brief account of the experimental setup and procedures, focus on the activity and deactivation of the WGS reaction in the different reaction atmospheres described below (Section 3.1). In the second part, we present in situ IR (diffuse reflectance FTIR spectroscopy—DRIFTS) data measured under the same conditions and in the same reaction atmospheres, providing insight into the build-up of adsorbed reaction intermediates and side products (Section 3.2). The effect of CO_2 and H_2O on the stability and decomposition behavior of the adsorbate layer present under steady-state conditions was further evaluated in transient DRIFTS experiments, following the variation in the adsorbate layer on sudden changes in the reaction atmosphere (Section 3.3). In the next two sections, we evaluate the influence of H_2 and CO_2 on the WGS reaction characteristics in more detail, first by determining the reaction order for these components (and also for CO and H_2O) in realistic reformate (Section 3.4) and then by characterizing the change in the adlayer during CO adsorption from a CO/N_2 mixture and during the WGS reaction in idealized reformate with stepwise increased H_2 content (Section 3.5). Finally, for characterizing the results of direct interaction of H_2 and CO_2 with the catalyst, we followed the build-up of the adlayer during the reverse water–gas shift (RWGS) reaction by DRIFTS (Section 3.6). The results are summarized in a comprehensive picture of the role of the different components on the deactivation process (Section 4).

2. Experimental

2.1. Catalyst preparation

The catalyst was prepared by deposition–precipitation as described previously [14,15]. In brief, the CeO_2 powder (HSA 15 from Rhodia, annealed in air at 400 °C for 2 h) was suspended in water at 60 °C at a pH of 6.5–7. To this suspension, tetrachloro auric acid ($HAuCl_4 \cdot 4H_2O$) was added under vigorous stirring while keeping the pH constant by adding Na_2CO_3 solution. After an additional 30 min of stirring, the precipitate was cooled to room temperature and filtered. The filtrate was suspended twice in warm water to reduce sodium and chloride contamination. After that, the precipitate was dried overnight at room temperature under vacuum. The Au metal loading (2.7 and 4.5 wt% Au) was determined by inductively coupled plasma atom emission spectroscopy (ICP-AES). The BET surface area of the catalysts was 188 m^2 g^{-1}. Before the experiments, the samples were conditioned in situ by first heating the raw catalyst to 230 °C (200 °C for the 2.7 wt% Au/CeO_2) in a

N_2 stream and keeping it there for 30 min, followed by a reduction in 10% H_2/N_2 at the same temperature for 45 min and a final N_2 treatment under similar conditions. Afterward, the sample was cooled down in N_2 to the reaction temperature.

2.2. Activity measurements

Activity measurements were carried out at atmospheric pressure in a quartz tube microreactor under differential reaction conditions, with typically 75–100 mg dilute catalyst powder. To limit the conversion to values typically between 5 and 20%, the catalyst was diluted with α-Al_2O_3, which is not active for the WGS reaction under the present conditions (for dilutions, see Table 1). The experiments were carried out with a gas flow of 80 Nml min^{-1} at 180 °C in the different gas mixtures specified above (for compositions, see Table 1). The gas mixtures were prepared by mass flow controllers (Hastings HFC-202). Defined amounts of water were added to the gas stream by passing it through a thermostatted water bath. Incoming and effluent gases were analyzed by on-line gas chromatography (Dani GC 86.10HT), using H_2 as carrier gas. High-purity reaction gases (CO 4.7, O_2 5.0, H_2 5.0, N_2 6.0, and CO_2 5.0; Westphalen) were used. The reaction rates were determined from the CO partial pressure; for further information on the measurements see Ref. [16]. Evaluation of the Weisz criterion showed the absence of mass transport-related problems [17].

2.3. Infrared measurements

In situ IR measurements were performed by DRIFTS using a commercial in situ reaction cell unit (Harricks, HV-DR2) [18]. The spectra were recorded in a Magna 560 spectrometer (Nicolet) equipped with a MCT narrow-band detector. Gas mixtures were prepared as described above, and similar gas flows were used (80 Nml min^{-1}). Between 40 and 50 mg of undiluted catalyst was used as a catalyst bed. Typically, 600 scans (acquisition time, 4.5 min; 400 scans for the 2.7 wt% Au/CeO_2 catalyst) were co-added for one spectrum. The intensities were evaluated in Kubelka–Munk units, which are linearly related to the adsorbate concentration [19]. Background subtraction and normalization of the spectra was performed by subtracting spectra recorded in a flow of N_2 at the reaction temperature directly after catalyst conditioning. To remove changes in the reflectivity (Figs. 2b and 7, and Supplementary material, Fig. S1b), the spectra were scaled to similar intensities aside the respective peaks. For evaluation of formate and CO_2 intensities, the spectra were adjusted to similar intensities at 2000 cm^{-1}; for evaluation of the carbonate region, the intensity at 950 cm^{-1} was used for calibration.

3. Results

3.1. Activity and deactivation measurements

3.1.1. Idealized reformates

In the first step, we investigated the influence of H_2 and CO_2 on the long-term stability of a 4.5 wt% Au/CeO_2 catalyst at 180 °C, comparing the decay in activity over 1000 min in the different gas mixtures, from dilute water–gas to $H_2 + CO_2$-rich idealized reformate (see Table 1). The resulting reaction rate–time relations are plotted in Fig. 1 as empty symbols. For better comparison, all curves were normalized to the respective initial activities (r_0); the absolute activities are listed in Table 1. In the idealized reaction mixtures, the activity drops nearly exponentially, whereas in the realistic reformate mixtures (1/4 realistic, 1/2 realistic, H_2-free realistic, and realistic reformate), the loss of activity is more pronounced in the later stages, after about 100 min (see below). The degree of deactivation differs significantly for the different gas mixtures. For reaction in idealized reformate, in dilute water–gas (1 kPa CO and 99 kPa N_2 (dry) + 2 kPa H_2O; Fig. 1, curve □), the catalyst exhibits a high initial activity for the WGS reaction (4.5×10^{-4} mol g_{Au}^{-1} s^{-1}; Table 1) and deactivates to about 79% of its initial activity over 1000 min. The deactivation behavior is strictly exponential. For reaction in H_2-rich idealized reformate (1 kPa CO and 99 kPa H_2 (dry) + 2 kPa H_2O; Fig. 1, curve ▽), we found a significantly lower initial reaction rate (2.2×10^{-5} mol g_{Au}^{-1} s^{-1}; Table 1), whereas the deactivation behavior did not change significantly (exponential decay, 77% activity after 1000 min). In contrast to H_2, adding 1 kPa CO_2 has a much more pronounced effect on the deactivation, resulting in a loss of activity to about 63% of the initial rate (exponential decay; Fig. 1, curve △ and Table 1). On the other hand, the effect on the absolute initial activity is much weaker (3.0×10^{-4} mol g_{Au}^{-1} s^{-1}; Table 1). If CO_2 and H_2 are added simultaneously to the idealized reformate, then deactivation is even more pronounced, and the activity decreases, in an exponential decay, to 56% of the initial activity (see Fig. 1, curve ◇ and Table 1). Hence, in the presence of 1 kPa CO_2 in the reaction gas, H_2 has a marked effect on the deactivation behavior, whereas in the absence of CO_2, in dilute water–gas, the addition of H_2 has little effect. The absolute initial activity in $CO_2 + H_2$-rich idealized reformate is signif-

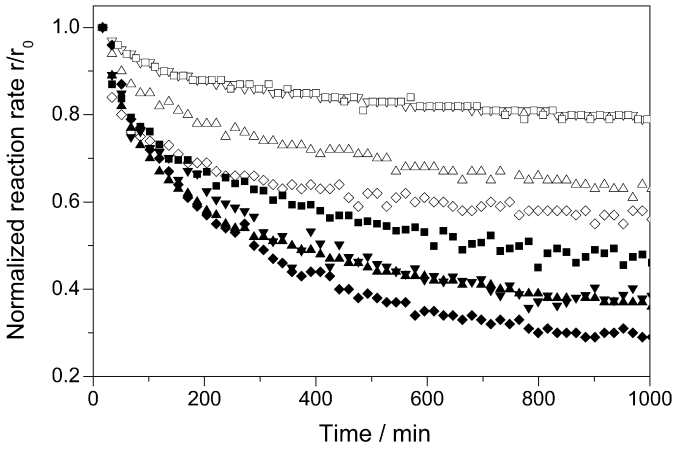

Fig. 1. Normalized reaction rate (r/r_0), where r_0 denotes the initial reaction rate, over a 4.5 wt% Au/CeO_2 catalyst at 180 °C as a function of reaction time, up to 1000 min in different reaction gas atmospheres (gas compositions see Table 1). Idealized reformate (□), H_2-rich idealized reformate (▽), CO_2-containing idealized reformate (△), $H_2 + CO_2$-rich idealized reformate (◇), 1/4 realistic reformate (■), 1/2 realistic reformate (▼), H_2-free realistic reformate (▲), realistic reformate (◆) (gas flow: 80 Nml s^{-1}).

Table 2
Reaction conditions and reaction atmosphere from previous studies on the deactivation of supported metal/CeO_2 catalysts during the WGS reaction

Catalyst	Reaction gas, partial pressures in kPa	Temperature (°C)	Time (h)	Deactivation (%)	Remarks	Reference
Au/CeO_2	CO: 2, H_2O: 20, rest He	360	48	83	Catalyst pretreatment: calcination in air at 500 °C for 5 h	[11]
Au/CeO_2	CO: 10, H_2O: 22, H_2: 43, CO_2: 6, rest N_2	240	12	65	Catalyst pretreatment: reduction in 4 kPa H_2 for 4 h	[6]
Au/CeO_2	CO: 7, CO_2: 11, H_2O: 38, H_2: 40, rest He	300	120	None		[21]
Au/CeO_2	CO: 5, H_2O: 15, H_2: 35, rest He	250	100	20		[7]
Au/CeO_2	CO: 5, H_2O: 31.1, rest Ar	140–350	504	None	Catalyst pretreatment in 1 kPa H_2 in Ar at 100 °C, 1 h	[13]
Pt/CeO_2	CO: 40, CO_2: 12, H_2: 60, H_2O: 120, N_2: 60	250	70	35	Deactivation rates independent of temperature, catalyst pretreatment: calcinations at 500 °C for 4 h	[9]
Pt/CeO_2	CO: 3, CO_2: 15, H_2: 48, N_2: 34 (dry); + H_2O: 26	150–350	70	Little	Decrease of CO conversion under shutdown/startup cyclical condition	[12]
Pd/CeO_2	CO: 3.3, H_2O: 3.3, rest He	250	12	Slow	Aging test, loss of the metal surface area, catalyst pretreatment: calcination in air at 650 °C	[10]

icantly lower than in CO_2-containing idealized reformate and comparable to that in H_2-rich idealized reformate; that is, the addition of 1 kPa CO_2 has little effect on the absolute initial activity. The negative effect of adding H_2 to the reaction atmosphere on the activity agrees well with the negative reaction order of H_2 (reaction order −0.5) in an idealized reaction atmosphere under similar conditions as reported by Leppelt et al. [5]. In contrast, the negligible effect of CO_2 on the initial activity does not correlate with the reaction order of −0.5 [5]. Here it should be kept in mind, however, that the reaction orders were measured under steady-state conditions, and thus the significant deactivation in the presence of CO_2 must be included. Comparing the activities after 1000 min shows that the presence of CO_2 also has a negative effect on WGS activity.

3.1.2. Realistic reformates

We investigated the activity and long-term stability of 4.5 wt% Au/CeO_2 at 180 °C in different realistic gas mixtures from 1/4 realistic to realistic reformate (see Table 1). The resulting reaction rate–time relations are plotted in Fig. 1 as filled symbols. The initial activities in realistic reformates follow the trends in idealized reformates, with a significant decay of the initial rate in the presence of H_2. Apparently, the much higher concentrations of CO and H_2O compared with those of the idealized reformates cannot suppress this effect, despite the positive reaction orders reported for these components [5]. Deactivation in the different realistic reformates is generally more pronounced and deviates from an exponential decay, with a stronger loss of activity after the initial phase (after about 100 min). The extent of deactivation increases with higher CO_2 concentration; 1/4, 1/2, and fully realistic reformate reduce the rate after 1000 min to about 46%, 38%, and 30% of the initial rate, respectively (Table 1). In H_2-free realistic reformate (Fig. 1, curve ▲), the deactivation is comparable to that in 1/2 realistic reformate (36% of the initial activity after 1000 min). Comparing the realistic reformate with and without H_2 shows an additional H_2-induced activity loss of 6%, which is of similar magnitude as the additional, H_2-induced activity loss in CO_2-containing idealized reformate (7% additional deactivation). The general observation that the presence of H_2 has little effect on deactivation seems to contradict the proposed overreduced ceria support as origin for the deactivation [9]. But it does not rule out a significant effect of support reduction on the WGS activity; in the present measurements, support reduction already occurs during the reductive conditioning procedure [5].

The deactivation behavior observed in the present experiments can be compared with that reported by Andreeva et al. [13], who found no deactivation of the Au/CeO_2 catalyst during the WGS reaction in idealized reformate (Table 2) over a wide temperature range (140–350 °C), and by Luengnaruemitchai et al. [11], who determined a pronounced deactivation by about 83% of the initial rate for a Au/CeO_2 catalyst for reaction at 360 °C in pure water–gas over a reaction time of 48 h. (After 1000 min of reaction, the deactivation was about 60%.) The apparent discrepancy between these results can be resolved when considering that in [13], the catalyst was pretreated at rather low temperatures (pretreatment in 1 kPa H_2 in Ar at 100 °C, 1 h), which likely cannot fully reduce the catalyst. In that case, continuing reduction of the catalyst during the reaction will counteract, and at least partly compensate for, deactivation of the catalyst. Furthermore, the high reaction temperature in [11] results in measurable growth of the Au particles, from 4 to 5.5 nm, which is responsible for at least part of the deactivation. (The still rather slow Au particle growth despite the high reaction temperature can be understood based on the pretreatment procedure, which involved calcination in air at 500 °C for 5 h.) Based on XPS and in situ DRIFTS measurements, Kim and Thompson reported the formation of carbonates and/or formates during the reaction (XPS) or during exposure of a H_2/CO mixture (DRIFTS) and proposed this as the source of the catalyst deactivation seen during reaction on Au/CeO_2 at 240 °C in realistic reformate (catalyst deactivation by ca. 65% over 12 h) [6]. Fu et al. reported a slight deactivation during 120 h of reaction at 300 °C on Au/CeO_2 catalysts with rather large Au particles (initial diameter, 4.8 nm) in realistic reformate [20,21]. They also observed growth of the Au particles from 5 nm to about 7 nm. However, according to the mechanistic model put forward by these authors, in which Au^0 acts only as a spectator [7,22], Au particle growth should not be responsible for the

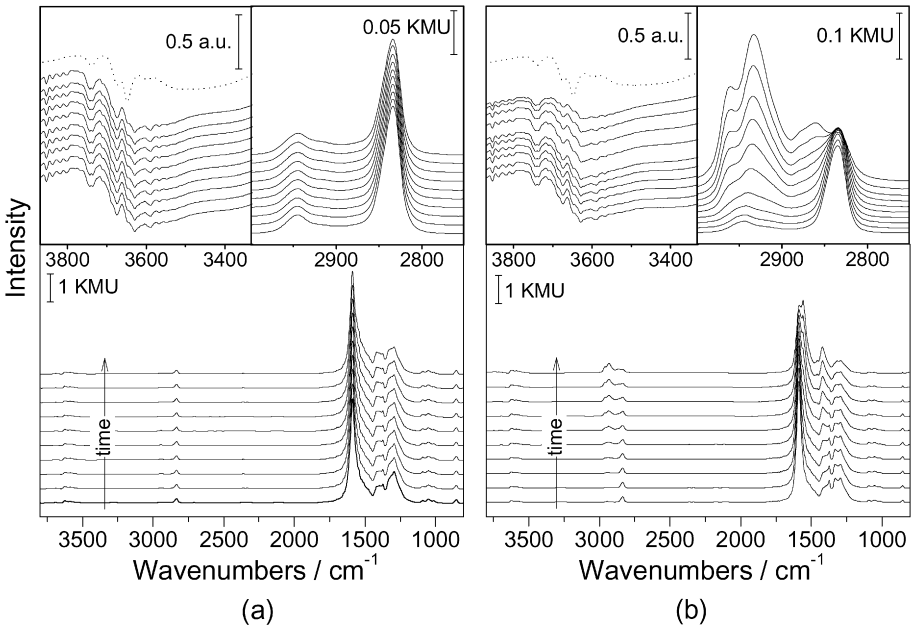

Fig. 2. Selected spectra from a series of DRIFT spectra recorded during the WGS reaction on an Au/CeO_2 catalyst at 180 °C in (a) idealized reformate and (b) H_2-rich idealized reformate (gas flow 80 Nml min^{-1}, 40–50 mg 4.5 wt% Au/CeO_2 catalyst, reaction times: 15, 30, 60, 120, 240, 360, 480, 600, 780, and 1020 min). Each panel shows the complete spectrum (bottom panel) as well as details of the O–H (top left panel; background: dotted curve) and C–H region (top right panel).

rather low catalyst deactivation (10–20% deactivation during the first 1000 min of reaction in CO_2-free reformate) [7]. Their results more closely agree with a carbonate/formate-based deactivation mechanism: due to the increased decomposition of these species at higher reaction temperatures, the deactivation should be less pronounced under these conditions than at lower reaction temperatures (see below). In total, the differences between our data and previous results can be readily explained by the different reaction conditions.

3.2. Deactivation—DRIFTS measurements

To characterize the build-up of the adsorbate layer under different reaction conditions, we performed in situ DRIFTS measurements under the same conditions as in the activity experiments, following the reaction until steady state was reached. The amount of catalyst used for the IR experiments is of the same order of magnitude as that used for the activity measurements, expect for those in idealized reformate and in CO_2-containing idealized reformate. For these conditions, a previous study found similar deactivation and activity behavior in the IR cell and in the microreactor [5]. Therefore, we can assume the same for the present study as well, allowing us to directly compare the IR measurements and the activity measurements in the microreactor. Sequences of representative IR spectra are displayed in Figs. 2a and 2b (idealized reformates) and Figs. 3a and 3b (realistic reformates). Both figures show the full spectra in the bottom panel and details of the spectral regions characteristic for O–H and C–H vibrations in the upper left and right panels, respectively. (Note that the figures show raw data for the O–H region to avoid artifacts caused by the pronounced changes in the background in this region.) The assignment of the different vibrational features follows those in previous studies, which are summarized in Table 3.

3.2.1. Idealized reformates

For reaction in idealized reformate (dilute water–gas), we find a rapid build-up of vibrational features associated with (gas phase) CO_2 (2363 and 2332 cm^{-1}), formates adsorbed on the ceria support with C–H vibrations at 2945 cm^{-1} (bridged formates) and 2833 cm^{-1} (bidentate formates), both antisymmetric and symmetric OCO bending vibrations, ν_{as}(OCO) and ν_s(OCO), at 1588 and 1374 cm^{-1} (shoulder) [23–25]. Well-separated peaks at 1420 and at 1291 cm^{-1} are related to monodentate and bidentate carbonates adsorbed on the ceria support, respectively [24,26], and peaks at 1291, 1051, and 850 cm^{-1} are attributed to the ν_{as}(OCO), ν_s(OCO), and ν_δ(OCO) vibrations of bidentate carbonates [24,26–28]. The ν(C=O) vibration of these species are expected at 1562–1610 cm^{-1} [25,27]; however, it is covered by the dominant formate peak at 1588 cm^{-1}. The other bands at 1420, 1334 (shoulder), and 1089 cm^{-1}, along with the band at 850 cm^{-1}, are related to monodentate carbonate species adsorbed on ceria or bulk carbonates [24,26,27,29]. Because we have no indication of a build-up of bulk carbonates, we have assigned these peaks to monodentate carbonates. The formation of bridged carbonates on the support, which should exhibit a characteristic vibration in the 1700–1750 cm^{-1} region [27], can be ruled out. Absorption features at 3647 cm^{-1} had been assigned to bridged OH_{ad} groups [24,30]. Finally, we also observed a peak at 3588 cm^{-1}, both in idealized and in realistic reformates, in agreement with observations reported by Leppelt at al. [5] for the WGS reaction in idealized reformate on a 2.6 wt% Au/CeO_2 catalyst, the exact origin of which has not yet been clarified.

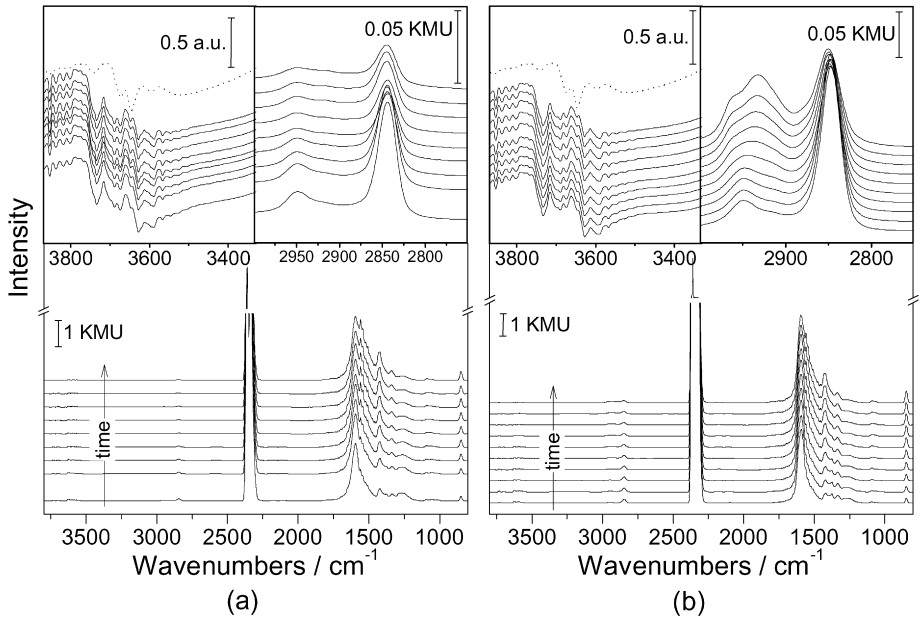

Fig. 3. Selected spectra from a series of DRIFT spectra recorded during the WGS reaction on an Au/CeO_2 catalyst at 180 °C in (a) H_2-free realistic reformate and (b) realistic reformate (gas flow 80 Nml min^{-1}, 40–50 mg 4.5 wt% Au/CeO_2 catalyst, reaction times: 15, 30, 60, 120, 240, 360, 480, 600, 780, and 1020 min). Each panel shows the complete spectrum (bottom panel) as well as details of the O–H (top left panel; background: dotted curve) and C–H region (top right panel).

Table 3
Peak positions reported of surface carbonate and formate species on CeO_2 and metal/CeO_2 catalysts

Species	Catalyst	Wave numbers (cm^{-1})	Reference
Monodentate carbonate	CeO_2	1454, 1348, 1062, 854	[26]
	CeO_2	1460, 1370, 1044	[24]
	CeO_2	1504, 1351	[28]
	CeO_2	1480–1460, 1380–1360, 1070, 850	[27]
	Rh/CeO_2	1460, 1390, 1060	[25]
Bidentate carbonate	CeO_2	1562, 1286, 1028, 854	[26]
	CeO_2	1570, 1286, 1028	[24]
	CeO_2	1567, 1289, 1014	[28]
	CeO_2	1610–1580, 1310–1250, 1030, 860–830	[27]
	Rh/CeO_2	1575, 1290, 1032	[25]
Bridged carbonate	CeO_2	1728, 1396, 1219, 1132	[26]
	CeO_2	1736, 1135	[28]
	CeO_2	1750–1700, 1180	[27]
Bulk carbonate	CeO_2	1462, 1353, 1066	[28]
	CeO_2	1480–1420, 1400–1350, 1060, 880	[27]
Formate species	CeO_2	2945, 2852, 1558, 1587, 1369, 1329 (two kinds of species)	[26]
	CeO_2	2840, 1585, 1563, 1358 (two kinds of species adsorbed on Ce^{3+})	[44]
	CeO_2	2840, 1550, 1358 (adsorbed on Ce^{4+})	[44]
Bidentate formate	CeO_2	2845, 1547, 1358	[24]
	Rh/CeO_2	2861, 1555, 1358	[25]
	Pt/CeO_2	2845, 1585, 1375	[30]
Bridged formate	CeO_2	2933, 1569, 1358	[24]
	Pt/CeO_2	2950, 1585, 1375	[30]

The formation and decomposition of the different adsorbate species during exposure to the reaction gas atmosphere can be illustrated by plotting the temporal evolution of the peak intensities together with the normalized reaction rate (r/r_0) (Fig. 4a). For these plots, we evaluated the intensities of the most significant peaks in the OCO region for monodentate carbonates (1420 cm^{-1}, △) and bidentate carbonates (1291 cm^{-1}, ▲), the bidentate formate related C–H signal at 2833 cm^{-1} (□), and the CO_2 related signal at 2363 cm^{-1} (○). We also included the reaction rate (●) normalized to an initial value of 1. At the beginning of the reaction (after 15 min), the intensities of adsorbed bidentate formats and bidentate carbonates, as well as

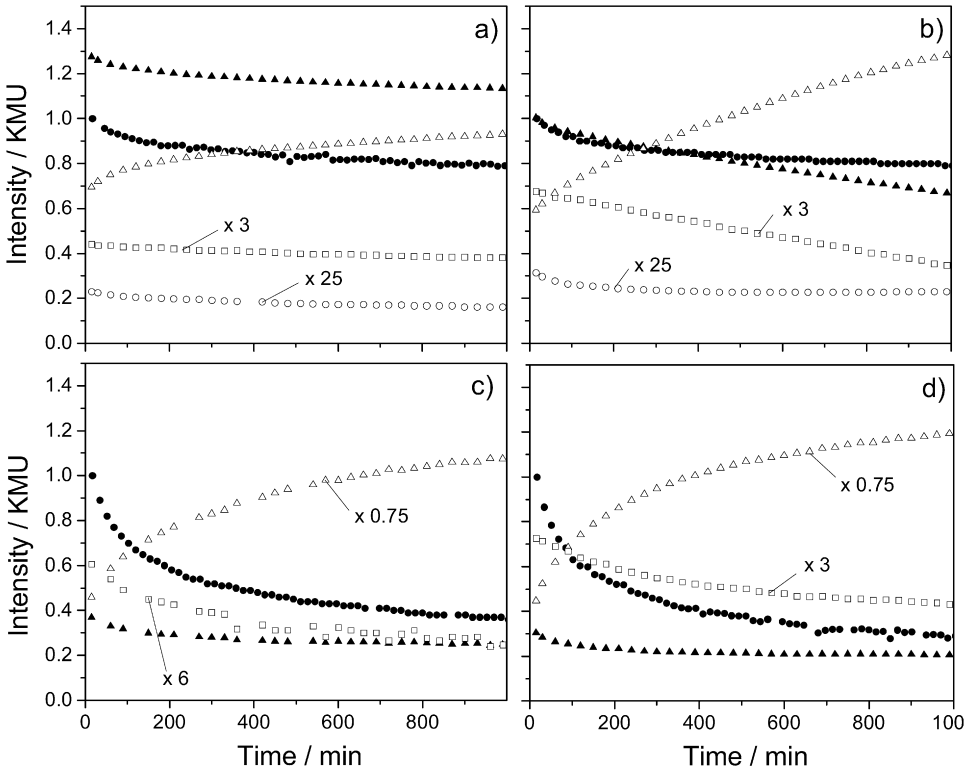

Fig. 4. Time development of the intensities of the characteristic peaks at 2833–2846 cm^{-1} (bidentate formate, □), 2363 cm^{-1} (CO_2, ○), 1420 cm^{-1} (monodentate carbonates, △), and 1287–1291 cm^{-1} (bidentate carbonates, ▲) as well as the normalized reaction rate (r/r_0) (●) during the WGS reaction on Au/CeO_2 over 1000 min in (a) idealized reformate, (b) H_2-rich idealized reformate, (c) H_2-free realistic reformate, and (d) realistic reformate (gas composition and spectra see Table 1 and Figs. 2 and 3).

the CO_2-related intensity, increase steeply, pass through a maximum, and then decrease slightly. The intensity of the CO_2 peak decays to 71% of the initial intensity during 1000 min of reaction time, closely fitting the deactivation observed in idealized reformate (decay to 79% of the initial rate; see Fig. 1 and Table 1). The intensities of the bidentate formate- and bidentate carbonate-related signals were reduced to about 86% and 89% of the initial value, respectively, after 1000 min of reaction. It should be noted that the steady-state coverage of adsorbed formates in idealized reformate (under similar reaction conditions) was found to be around 0.3 mL (relative to the total oxide surface area) [5]. Moreover, the decay of the bidentate formate, the CO_2 intensity, and the reaction rate show similar characteristics, in agreement with findings by Leppelt et al. [5]. Monodentate carbonates are formed during the reaction and steadily increase in intensity (Fig. 4a, peak increase by 32% during 1000 min of reaction). We later (Section 3.3) show that these surface carbonates are rather stable and that deactivation of the catalyst is correlated with the build-up of monodentate carbonates, which apparently can block active sites and thus inhibit the reaction of CO_{ad} with OH groups to formate.

In H_2-rich idealized reformate (Fig. 2b), the general appearance of the spectra is quite similar to that in (H_2-free) idealized reformate (Fig. 2a): at the beginning of the reaction (after 15 min) formate formation is indicated by peaks at 2944, 2835, 1588, and 1373 cm^{-1} (weak), similar to the trend in idealized reformate. After 60 min of reaction, these peaks decrease in intensity, and new peaks at 2960, 2933, 2861, and 1558 cm^{-1} emerge. After 1000 min of reaction time, the latter features dominate the spectrum. Following previous reports, we have assigned the peaks at 2861 and 1558 cm^{-1} to bidentate formate species [24,25,30]. The shift in wavenumber is attributed to the change in surface oxidation state, providing different surface species (e.g., Ce^{3+} instead of Ce^{4+}). The signals at 2960 and 2933 cm^{-1}, which appear only in H_2-rich atmosphere, where Ce^{4+} can be reduced to Ce^{3+}, are attributed to bridged formate species, possibly on Ce^{3+} and Ce^{3+}/Ce^{4+} sites. The formation of monodentate formates can be excluded from the absence of the characteristic peak at 1620 cm^{-1} for the ν(C=O) vibration [28]. Furthermore, we also observed bidentate (1291 cm^{-1}) and monodentate (1420 cm^{-1}) carbonates. Interestingly, the intensity of the bidentate carbonates decreases to 66% during 1000 min of reaction, whereas that of the monodentate species increases to 217% (see Section 3.3). The intensity of the CO_2 peak decays to 73% of the initial value during 1000 min of reaction, which is in the same range as expected from the activation, is similar to that in idealized reformate (Fig. 1 and Table 1), the decrease in CO_2 intensity should be, and is, in the same range as that in idealized reformate. On the other hand, the intensity loss of the bidentate formate-related signal, which decreases to about 50% of the initial value after 1000 min of reaction, is much stronger than in idealized reformate. We assume that this discrepancy originates from a modification of the ceria substrate surface, which affects the relation between bidentate formate coverage and CO_2 formation rate. Finally, catalyst deactivation is accompanied by an increase in the monodentate

carbonate species, again pointing to a reaction-inhibiting role of this species (see above).

The spectra and their characteristic features of CO_2-containing idealized reformate (see Supplementary material, Figs. S1a and S3a) generally resemble those in idealized reformate, with a small shift in the bidentate formate-related peak in the C–H region, which now appears at 2838 cm^{-1}. The changes in the peak intensities during the reaction are more pronounced (Table 4) than in idealized reformate, with the formate- and bidentate carbonate-related signals decreasing to about 80% and 87% of their initial value, respectively, during 1000 min of reaction. Due to the high gas-phase CO_2 concentration, we could not plot the CO_2 intensity. The monodentate carbonate increases by 51% during 1000 min of reaction. These carbonates are a suggested origin for catalyst deactivation, which we discuss in more detail in Section 3.3

In an $H_2 + CO_2$-rich atmosphere (see Supplementary material, Figs. S1b and S3b), the spectra seem to be dominated by the presence of H_2 and are largely similar to those in H_2-rich idealized reformate (Fig. 2b), with formate peaks at 2946, 2841, 1590, and 1374 cm^{-1} (weak) at the beginning of the reaction. After 60 min of reaction time, additional formate species build up, with peaks at 2961 (shoulder), 2933, 2855, and 1559 cm^{-1} (shoulder). The latter features increase and dominate the spectrum after 1000 min of reaction. The intensities of the bidentate formate-related signals were reduced to about 34% of the initial value after 1000 min of reaction. The intensity of bidentate carbonates decreased to about 43% and that of monodentate species increased by about 117% during the reaction (Table 4). Thus, the increase of monodentate carbonate-related intensity is significantly higher (about twice as high) than in the absence of H_2 in CO_2-rich idealized reformate.

Comparison of the activity measurements with the DRIFTS data leads to the following conclusions:

1. In H_2-free atmosphere, the deactivation correlates with an increasing build-up of the monodentate carbonate.
2. In CO_2-containing atmosphere, the increase in monodentate carbonate and decrease in bidentate formate are more pronounced than that in dilute water–gas. More monodentate carbonates are built up when CO_2 is present, which also occurs in realistic reformates (see below). It seems that part of the monodentate carbonates adsorbs on active sites, which can inhibit the reaction of CO_{ad} and OH groups to formate or block adsorption sites for CO adsorption on the support (decrease in the capture zone for CO adsorption [5]). This results in a stronger decrease of the formate species on the catalyst, as well as in stronger deactivation.
3. In an H_2-rich atmosphere, the amount of deactivation is the same as in idealized water–gas, although the coverage decrease of the bidentate formate species is much more pronounced. In addition, the formate peak shifts to higher wavenumbers during the reaction, reflecting a stronger C–H bond. On the other hand, there is also a pronounced increase in the bridged formate intensity, contrasting the behavior in an idealized reformate in which the coverage of this species remains virtually constant. A possible reason for the partial conversion of the formate species on Au/CeO_2 during the water–gas shift reaction in H_2-rich idealized atmosphere could be an increasing reduction of the support from Ce^{4+} to Ce^{3+}. Together with a lower formation of coadsorbed OH_{ad}, this leads to changes in the chemical properties and hence the adsorption behavior of the ceria surface. If formate decomposition is rate-limiting, than the bridged formates must be less active or more stable for CO_2 formation than the bidentate formates, but still reasonably active to explain the present results.
4. In $CO_2 + H_2$-rich reformate, we observed a similar conversion from bidentate to bridged formates as in H_2-rich atmosphere, but a much more pronounced deactivation. This trend supports a mechanistic interpretation in which the monodentate carbonate species, which are formed in both CO_2-containing and $H_2 + CO_2$-rich atmospheres, are mainly responsible for the deactivation, rather than the formate species. This is the topic of Section 3.3.

3.2.2. Realistic reformates

Similar in situ DRIFTS experiments as described above were performed in the realistic reformate mixtures (Figs. 3a and 3b) and presented in the same way (full spectra in the bottom panel; details of the O–H and of the C–H region in the top left and top right panels, respectively). The related integrated intensities are plotted in Figs. 4c and 4d. Because of the high CO_2 contents in the reaction gas, variations in CO_2 intensity could not be evaluated and were not plotted.

In realistic reformate (Figs. 3b and 4d), the general characteristics of the spectra are similar to those in idealized reformate (Fig. 2a), with the following changes:

(i) The bidentate formate peak is shifted to 2850 cm^{-1} (idealized reformate at 2833 cm^{-1}), but, in contrast to the reaction in H_2-rich idealized reformate, a peak shift did not occur during the reaction. Apparently, the reduction of the support is partly compensated by water.

(ii) The build-up of bridged formates during the reaction, which we also found in H_2-rich idealized reformate, is found in all reaction atmospheres.

(iii) OH intensities are generally higher in the realistic reformates than in the idealized reformate (Fig. 2a), due to the higher water concentration. As expected from the tendencies in H_2-rich and CO_2-rich gases, the changes in peak intensities during deactivation increase further (Fig. 4d and Table 4) compared with those in idealized and CO_2-containing idealized reformate. The intensities of the bidentate formate- and bidentate carbonate-related signals decrease to about 60% and 67% of the initial value, respectively, after 1000 min of reaction. Finally, based on the IR intensities, the total amount of the reactive bidentate formates is of similar order of magnitude as in idealized reformate (0.3 mL; see Section 3.2.1 and [5]). The intensity of the bridged formate is lower than in H_2-rich or $H_2 + CO_2$-rich idealized reformate. Most importantly, the increase in monodentate carbonate peak intensity is much

Table 4
Change of the peak intensities/integrated intensities/integrated intensities (peak fit) over 1000 min WGS reaction in various idealized and realistic reformates

Reaction gas mixture	CO_2 concentration (kPa)	Bidentate formate (2833–2846 cm^{-1}) (%)	Monodentate carbonate (1419–1421 cm^{-1}) (%)	Bidentate carbonate (1287–1291 cm^{-1}) (%)	CO_2 (2363 cm^{-1}) (%)	Activity (GC) after 1000 min (%)
Idealized reformate	0	86	134	89	71	79
H_2-rich ideal. reformate	0	50	217	66	73	77
CO_2-cont. ideal. reformate	1	80	151	87	–	63
$H_2 + CO_2$-rich ideal. reformate	1	34	217	43	–	56
1/4 realistic reformate	4.2	77	199	74	–	46
1/2 realistic reformate	8.4	74	239	71	–	38
H_2-free realistic reformate	16.8	42	235	67	–	36
Realistic reformate	16.8	60	268	67	–	30

Note. The activity/intensity after 15 min reaction is set to 100%. The values given describe the remaining intensity after 1000 min on stream.

stronger than in idealized reformates, by about twofold during 1000 min of reaction.

In the 1/4 realistic and 1/2 realistic reformate (see Supplementary material, Fig. S2 (a and b) and Fig. S3 (c and d)), the trends are similar, but the changes are less pronounced due to the lower partial pressure of CO, CO_2, H_2, and H_2O. The bidentate formate peaks appear at slightly lower frequencies (2842 and 2846 cm^{-1}, respectively), instead of 2850 cm^{-1} in realistic reformate. In addition, fewer bridged formates are built up at the lower partial pressures. The decrease in bidentate formate and increase in monodentate carbonate coverage are less pronounced than in realistic reformate, but stronger than in idealized reformates. This agrees well with the increasing catalyst deactivation compared with that in idealized reformate (Fig. 1), and supports our proposal that the catalyst deactivation is due mainly to the presence of monodentate carbonates. In contrast to the H_2-free gas mixtures, the amount of bidentate carbonates is much lower in realistic reformates, and monodentate carbonates are the main carbonate species on the support.

The general characteristics of the spectra in H_2-free realistic reformate (Figs. 3a and 4c) are similar to those in idealized and CO_2-containing idealized reformate. Only the bidentate formate is shifted to 2845 cm^{-1}. The intensities of bidentate formate and bidentate carbonate decrease to 42% and 67%, respectively, whereas that of monodentate carbonate increases to 235%. This increase is much more pronounced than that in CO_2-containing idealized reformate. The greater increase in monodentate carbonates, which results in a correspondingly increased site blocking on the support, agrees well with the observed stronger deactivation.

To better illustrate the correlation between formate/carbonate deposits and deactivation, we have summarized the change in the relative intensities of monodentate and bidentate carbonates, bidentate formats, and kinetic deactivation (GC) after 1000 min of reaction, as well as the CO_2 concentration in the respective gas mixtures in Table 4. The data show a clear correlation between increasing deactivation and increasing monodentate carbonate formation and decreasing CO_2 concentration in the reaction gas. Furthermore, the adsorbed carbonates seem to reduce the amount of bidentate formates. On the other hand, bridged formates are built up in reaction gas mixtures with high H_2 partial pressure ($p_{H_2} > 78$ kPa), most likely related to an increasing reduction of the support due to the higher H_2 partial pressure compared with the reductive pretreatment [5]. Similar to the behavior in idealized reformates, we tentatively conclude that the bridged formats (the coverage of which increases significantly during the reaction) do not influence the deactivation behavior (see Section 3.3). As mentioned earlier, the bridged formates must be active for CO_2 formation as well, but less active than the 2833 cm^{-1} bidentate formates.

3.3. Transient DRIFTS measurements

The stability of the steady-state adlayer on changes in the reaction atmosphere and the resulting modification of the adlayer were investigated in transient experiments after the changes in the adlayer by continuous DRIFTS measurements. In the first experiment, we investigated the effect of CO_2 on the adlayer and on the reaction characteristics, in particular of the formate species formed in idealized reformate when changing from (CO_2-free) idealized reformate to CO_2-containing idealized reformate (Fig. 5). To achieve steady-state conditions, the catalyst was first exposed to idealized reformate at 180 °C for 1225 min. This first part of the experiment is identical to the sequence shown in Fig. 2a. Subsequently, 1 kPa of CO_2 was added to the reaction gas. The first spectrum was recorded during the first 5 min after adding CO_2. Representative spectra and details recorded during this experiment are collected in Fig. 5a. Intensity–time profiles of the characteristic vibrational peaks at 2363 and 2332 cm^{-1} (CO_2), 2833 cm^{-1} (bidentate formate), 1420 cm^{-1} (monodentate carbonate), and 1291 cm^{-1} (bidentate carbonate) are plotted together with the normalized CO_2 formation rate in Fig. 5b.

Adding CO_2 to the gas mixture does not produce any significant changes in the peak positions, but does do so in the peak intensities (see Fig. 5b). The amount of surface formates (2833 cm^{-1}) decreases, and the peaks related to surface carbonates (1291 and 1420 cm^{-1}) grow in intensity. The increase in bidentate carbonate is attributed to a higher formation rate of these species, caused by the higher partial pressure of CO_2. With addition of CO_2, the intensities of formate (Fig. 5b, □) and bidentate carbonate (Fig. 5b, ▲) decreased by about 8%

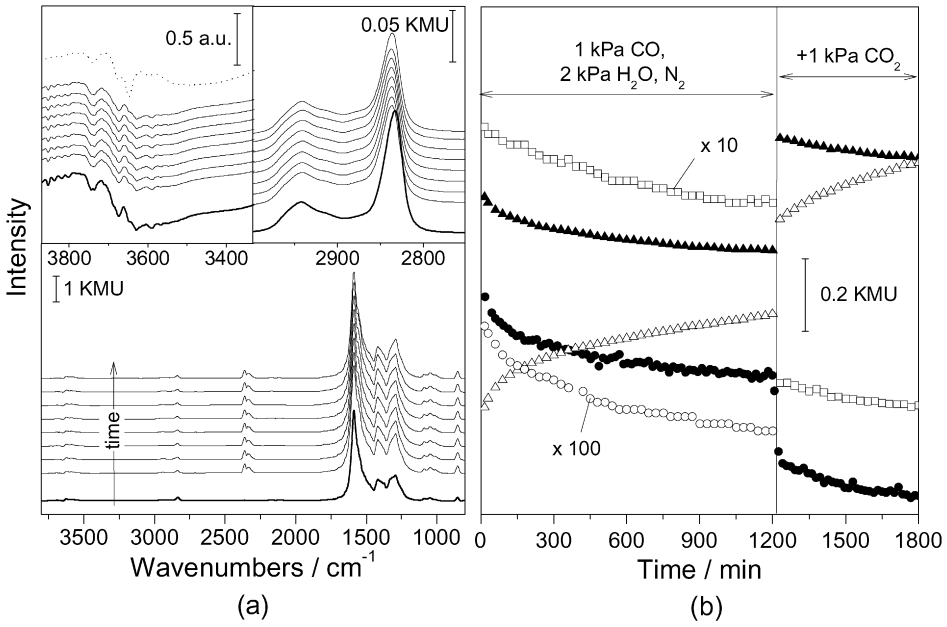

Fig. 5. (a) Selected spectra from a series of DRIFT spectra recorded during WGS reaction on a 4.5 wt% Au/CeO_2 catalyst at 180 °C upon changing from idealized reformate to a 1 kPa CO_2 containing gas mixture (CO_2-containing idealized reformate) over 600 min reaction (1230–1830 min; fine lines: 1230, 1260, 1290, 1350, 1470, 1590, 1710, and 1830 min). Prior to this reaction steady state in idealized reformate was obtained by reaction over 1225 min (0–1225 min; bold curve: 1200 min) under similar conditions. Bottom panel: complete spectra; top left panel: detail spectra of the O–H region (dotted line: background); top right panel: detail spectra of the C–H stretch region. (b) Temporal evolution of the integrated peak intensities at 2833 cm^{-1} (bidentate formate, □), 2363 cm^{-1} (CO_2, ○), 1420 cm^{-1} (monodentate carbonate, △), 1291 cm^{-1} (bidentate carbonate, ▲), and normalized reaction rate (r/r_0) (●) during the reaction.

and 4% of the initial values, respectively, after 510 min. Here the first spectrum after CO_2 addition (at 1230 min in Fig. 5b) was taken as the initial value. This intensity increase contrasts with the trend seen during deactivation in idealized reformate, with formate and bidentate carbonate intensity decreases of about 4% and 2%, respectively, of the intensity after 690 min (510 min before the change in reaction gas). (Here we compare the deactivation behavior during 510 min before and after the change from idealized reformate to CO_2-containing idealized reformate, because for a similar deactivation behavior in both atmospheres, deactivation before the change would be expected to be greater than after that change.) On the one hand, the deactivation behavior after change fits well with the enhanced deactivation caused by CO_2 in the reaction gas, where the reaction rate decreases twice as much in CO_2-containing idealized reformate as in idealized reformate, by 12% of the value at $t = 1230$ min over 510 min, compared with 4% during the last 510 min in idealized reformate. On the other hand, the carbonate intensity increases twice as fast in the presence of 1 kPa CO_2 (CO_2-containing idealized reformate) as in the absence of CO_2 (idealized reformate), from a 6% increase in the last 510 min before CO_2 addition to 12% over 510 min after CO_2 addition. This observation of stronger carbonate accumulation and decay in bidentate formate coverage in the presence of CO_2 in combination with a more pronounced deactivation, agrees well with our previous proposal that under present reaction conditions, the formation of surface carbonates is responsible for catalyst deactivation due to site blocking on the support surface. In this way, carbonate formation results in a simultaneous decay of the bidentate formate coverage. Overall, these observations also agree with our previous proposal that bidentate formate decomposition is the rate-limiting step of the WGS reaction [5].

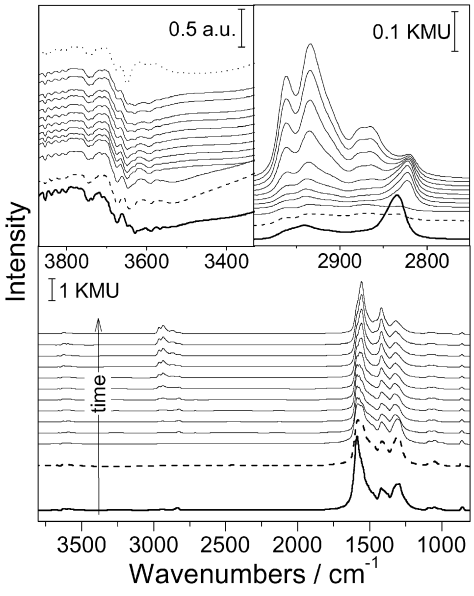

Fig. 6. Selected spectra from a sequence of DRIFTS spectra recorded during reaction of a surface carbonate saturated 4.5 wt% Au/CeO_2 catalyst with H_2 at 180 °C (fine lines: 0, 15, 30, 60, 120, 240, 360, 480, 600, 780, and 1020 min). Bottom panel: complete spectrum, top left panel: detail spectra of the O–H region (dotted line: background), top right panel: detail spectra of the C–H region. Carbonate saturation was obtained by preceding reaction in idealized reformate (bold curve) and subsequent 60 min flushing with N_2 at 180 °C (dashed curve).

In a second transient experiment, we investigated the possibility of a reaction between H_2 and surface carbonates. This was

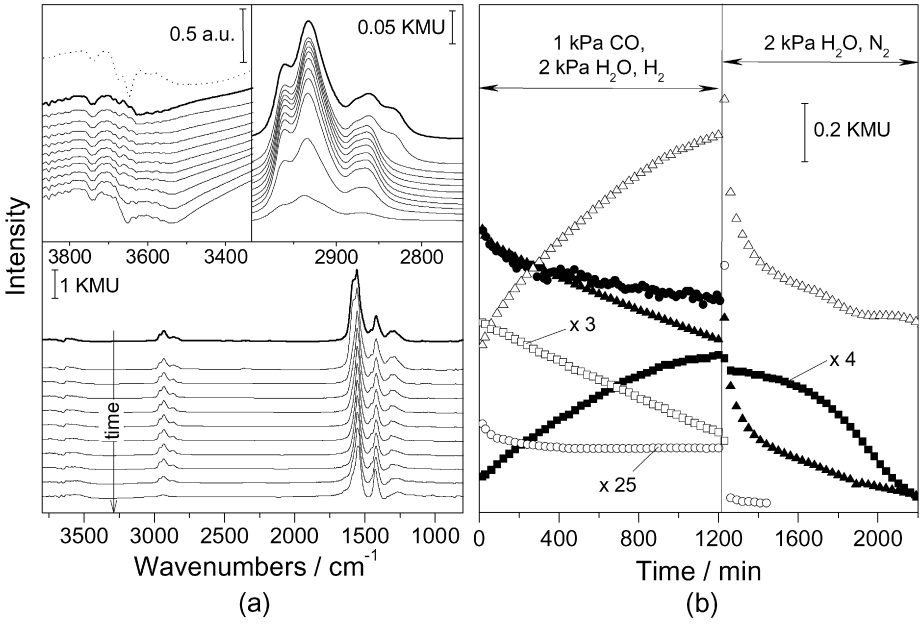

Fig. 7. (a) Selected spectra from a sequence of DRIFT spectra recorded during WGS reaction on Au/CeO_2 at 180 °C in H_2-rich idealized reformate (0–1225 min, bold curve: 1200 min) and subsequent change to 2 kPa H_2O in N_2 (1230–2250 min, fine curves: 1230, 1260, 1290, 1350, 1470, 1590, 1710, 1830, 2010, and 2250 min). Bottom panel: complete spectra; top left panel: detail spectra of the C–H stretch region; top right panel: detail spectra of the OCO bending region. (b) Temporal evolution of the intensities of the characteristic peaks at 2833 cm^{-1} (bidentate formate, □), 2861 cm^{-1} (bidentate formate, ■), 2363 cm^{-1} (CO_2, ○), 1420 cm^{-1} (monodentate carbonate, △), 1291 cm^{-1} (bidentate carbonate, ▲), and normalized reaction rate (r/r_0) (●) during the reaction.

done by first preparing a carbonate-saturated catalyst surface by reaction in idealized reformate (see Fig. 2a) and subsequent flushing with N_2 (60 min, 180 °C) to remove the reaction gas and to decompose the adsorbed formate species, followed by exposure to a H_2 stream (Fig. 6). After N_2 flushing, the surface contained only mono- and bidentate carbonates and OH_{ad} groups. On exposure to H_2, bidentate formate species reappeared, with a C–H frequency (2822 cm^{-1}) slightly lower than that of similar species created during reaction in idealized reformate. On further H_2 exposure, bidentate formate species at 2864–2877 cm^{-1} and bridged formates at 2934 and 2961 cm^{-1} appear, and the initial formate species (2822 cm^{-1}) decays in intensity. Because of the absence of CO and CO_2 in the gas phase, these new formate species must result from reduction of the bidentate carbonates, which decrease in intensity during reaction with H_2. In contrast, the intensity of monodentate carbonates remains about constant. These results provide a simple explanation of our earlier observation of low bidentate carbonate coverage and a lower tendency for deactivation in H_2-rich reaction gases (see Section 3.2).

In a third transient experiment, we investigated the stability and reactivity of bridged formates. For this experiment, the surface was first saturated with these species by reaction in H_2-rich idealized reformate (formate build-up, 0–1200 min). The adsorbates, including the bridged formates, were then (partly) decomposed in a CO-free 2 kPa H_2O/N_2 gas mixture (formate decomposition, 1200–2200 min) (see Fig. 7). As discussed in Section 3.2, the initially produced bidentate formate (2833 and 1588 cm^{-1}) decayed after 60 min, and different bidentate (2861 cm^{-1}) and bridged formate species (2933 and 2960 cm^{-1}) were built up. Changing to the CO-free atmosphere, the 2833 cm^{-1} formate species indeed disappeared quickly, completely vanishing after 30 min; in contrast, the decomposition of the other formate species was much slower, completed after 1200 min. A similar decay was observed for the bidentate carbonates (1291 cm^{-1}). In contrast, the monodentate carbonates (1420 cm^{-1}) are more stable, with an intensity loss of only about 50%. These results of different carbonate stabilities agree closely with previous reports on the thermal stability of carbonates on CeO_2 [26,28,31–34]. It should be noted that the much faster decomposition of carbonates on a Pt/CeO_2 catalyst in H_2O-containing atmosphere reported by Hilaire et al. [35] referred to measurements at 400 °C.

The latter experiment clearly demonstrates that the low-frequency 2833 cm^{-1} formate species are much less stable than the other bidentate and bridged formate species, and that monodentate carbonates are by far the most stable adsorbate on the catalyst. The 2833 cm^{-1} formate species is the same as that observed during reaction in idealized reformate, the decomposition of which had been identified as rate-limiting in the WGS reaction under those conditions [5].

3.4. Reaction kinetics in realistic reformate

The influence of CO_2 and H_2 on the WGS reaction was further investigated by determining the reaction orders for CO, H_2O, CO_2, and H_2. This was done by varying the partial pressure of one component while keeping the other components constant. The differences were compensated for with N_2. The measurements were performed on a 4.5 wt% Au/CeO_2 catalysts (reductive conditioning; see Section 2.1), after running the reaction over 1000 min in realistic reformate and waiting for at least 60 min at each gas composition until quasi-steady-state

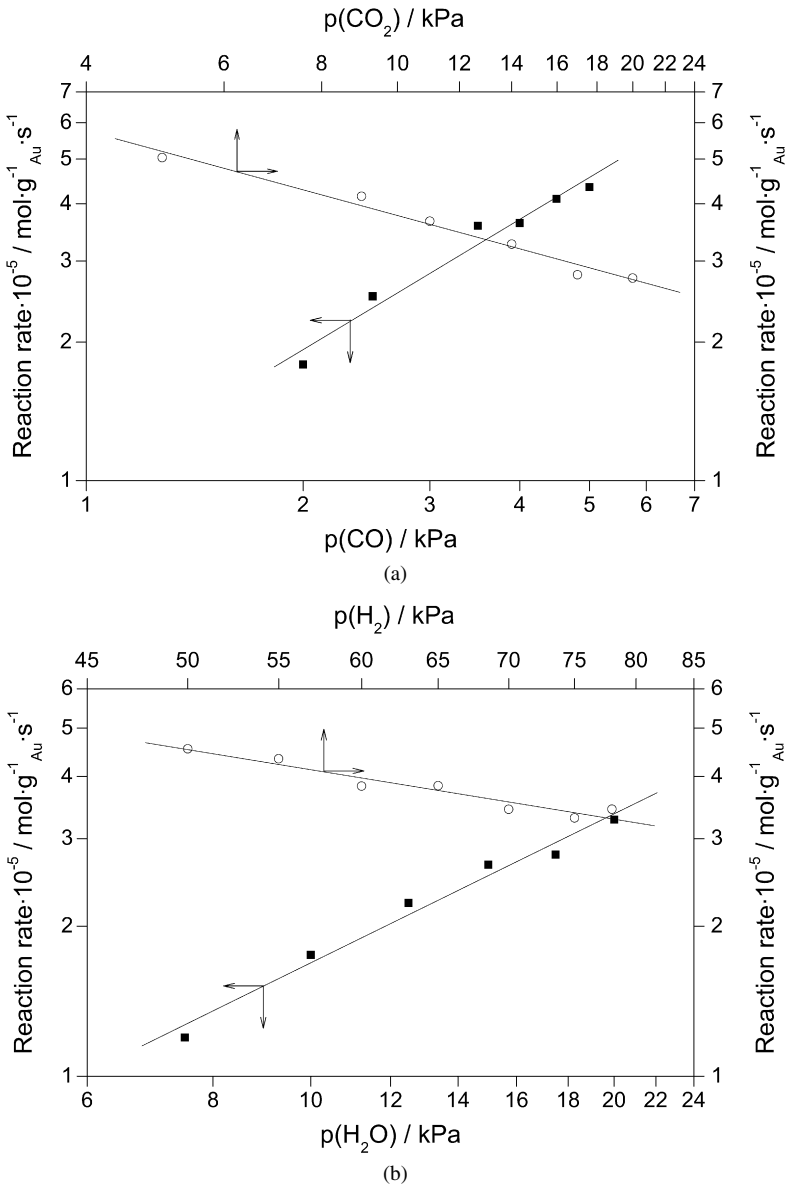

Fig. 8. Determination of the reaction order of (a) CO (2–5 kPa CO) and CO_2 (5–20 kPa CO_2); (b) H_2O (5–20 kPa H_2O) and H_2 (50–78 kPa H_2) on a 4.5 wt% Au/CeO_2 catalyst at 180 °C in realistic reformate (4 kPa CO, 16.8 kPa CO_2, 68.2 kPa H_2 (dry) + 20 kPa H_2O, 80 Nml min^{-1}). Changes in the gas composition were compensated by N_2.

conditions were reached. The results are presented in Fig. 8 and Table 5. The reaction order for CO and H_2O are both 1.0 ± 0.1 (Figs. 8a and 8b). For CO_2 and H_2, the reaction orders are -0.5 ± 0.1 and -0.7 ± 0.1 (see Figs. 8a and 8b), respectively (for gas compositions, see Table 5).

To date, measurements of the WGS reaction orders on a Au/CeO_2 catalyst in realistic reformate have not been reported. Leppelt et al. [5] determined reaction orders of 0.5 for CO and H_2O in idealized reformate (only CO and H_2O in N_2) over Au/CeO_2 and found that the presence of the other components in realistic reformate results in significantly enhanced effect of CO and H_2O partial pressures on the WGS reaction rates. From measurements in CO_2-containing and H_2-rich idealized reformate, these authors also determined reaction orders of -0.5 for both CO_2 and H_2 on Au/CeO_2 [5], identical to our present results. Apparently, the effect of these reactants on the reaction rate is not modified by the varying composition of the reaction gas mixtures in both experiments.

In comparisons with other ceria-supported noble metal catalysts, Koryabkina et al. [36] reported reaction orders of 0.9 and 0.4 for CO and H_2O in realistic reformate (for gas composition, see Table 5) on an 8 wt% CuO/CeO_2 catalyst and of -0.6 for CO_2 and H_2. Hilaire et al. [37] derived reaction orders of 0 for CO, 0.5 for H_2O, -0.5 for CO_2, and -1 for H_2 in dilute water–gas on Pd/CeO_2. For reaction on ceria-supported Pd, Pt, and Rh catalysts, Bunluesin et al. obtained reaction orders of 0 for CO and 1 for H_2O [38].

The high reaction order for CO on the Au catalysts, which contrasts with the results on other supported noble metal catalysts, can be explained by the weak interaction between CO and Au. This leads to an increased steady-state CO_{ad} coverage with increasing CO partial pressure on the Au catalysts.

Table 5
Reaction orders for the WGS reaction on noble metal/CeO_2 catalysts and related reaction conditions

Catalyst	Reaction gas (kPa)	Temperature (°C)	Reaction order	Reference
Au/CeO_2	CO: 2–5, CO_2: 16.8, H_2: 68.2, rest N_2 (dry); H_2O: 20	180	1.0 ± 0.1	This work
	CO: 4, CO_2: 16.8, H_2: 68.2, rest N_2 (dry); H_2O: 5–20		1.0 ± 0.1	
	CO: 4, CO_2: 5–20, H_2: 68.2, rest N_2 (dry); H_2O: 20		-0.5 ± 0.1	
	CO: 4, CO_2: 16.8, H_2: 50–78, rest N_2 (dry); H_2O: 20		-0.7 ± 0.1	
Au/CeO_2	CO: 0.2–2, H_2O: 2, rest N_2	180	0.5 ± 0.1	[5]
	CO: 1, H_2O: 0.7–10, rest N_2		0.5 ± 0.1	
	CO: 1, H_2O: 2, CO_2: 1.2–3.4, rest N_2		-0.5 ± 0.1	
	CO: 1, H_2O: 2, H_2: 3.2–75, rest N_2		-0.5 ± 0.1	
CuO/CeO_2	CO: 5–25, H_2O: 22, H_2: 37; CO_2: 8.5, rest Ar	240	0.9	[36]
	CO: 7, H_2O: 10–46, H_2: 37; CO_2: 8.5, rest Ar		0.4	
	CO: 7, H_2O: 22, H_2: 37; CO_2: 5–30, rest Ar		−0.6	
	CO: 7, H_2O: 22, H_2: 25–60; CO_2: 5–30, rest Ar		−0.6	
Pd/CeO_2, Pt/CeO_2, Rh/CeO_2	CO: not mentioned, H_2O: 2, rest N_2	300	0	[38]
	CO: 2.7, H_2O: not mentioned, rest N_2		1	

For other noble metal catalysts, in contrast, the CO adlayer is already close to saturation, so that a further increase in CO partial pressure does not lead to an increase in reaction rate. The higher CO reaction order in realistic reformate compared with idealized reformate is tentatively attributed to co-adsorption of hydrogen on Au [39]. Also, the high reaction order of H_2O can result from the competition between H_2 and H_2O for adsorption sites (see Section 3.5).

The negative CO_2 reaction order can be explained by different effects, most simply by the increasing reverse WGS reaction, but also by an increasing blocking of ceria surface sites and possibly also of active sites with surface carbonate. Within the limits of these measurements, the H_2 and CO_2 reaction orders do not reveal significant differences between reaction in realistic and idealized reformate [5]. Because in realistic reformate the reaction orders were determined in the presence of the respective other component, whereas this was not the case for the determination in idealized reformate (see Table 5), we conclude that the reaction characteristics are not altered by the presence of CO_2 and H_2, in contrast to their effect on the reaction rate and deactivation behavior.

Overall, these measurements in realistic reformate show a much more pronounced dependence of the activity on the reactant concentration than has been observed in idealized gas mixtures, along with decreased activity for noble metal/ceria systems if CO_2 and H_2 are in the gas mixture.

3.5. Influence of H_2 on CO adsorption and the WGS reaction

To further elucidate the influence of hydrogen on the adsorption and reaction behavior of CO on the Au/CeO_2 catalysts, we investigated the CO adsorption behavior in gas mixtures containing constant amounts of CO and increasing amounts of H_2 (0.5 kPa CO, 0–97 kPa H_2, balance N_2) on a 2.7 wt% Au/CeO_2 catalyst at 180 °C by DRIFTS. Spectra obtained under steady-state conditions after at least 4 h adsorption are shown in Fig. 9, left panel (bottom panel: full spectra; upper left panel: detailed spectra of the C–H region; upper right panel: detailed spectra of the CO region). CO adsorption in N_2 leads to a peak at 2097 cm^{-1}, which is commonly assigned to CO adsorbed on the Au particles [40]. Raising the H_2 partial pressure stepwise from 0 to 97 kPa shifts the CO band from 2097 to 2116 cm^{-1}. (Note that for these experiments, a freshly conditioned catalyst was used for each H_2 concentration.) It also significantly reduces the intensity. We assume that the shift to higher wavenumbers is caused by co-adsorption of hydrogen on Au [39]. In addition to the CO_{ad}-related signal, two peaks at 2845 and 2950 cm^{-1} appear in the C–H stretching region in the absence of H_2, which are characteristic for bidentate formates [5]. These formates are formed by reaction of CO_{ad} and OH_{ad} [23,41], with the latter species remaining on the support after the reductive pretreatment [42]. Further formation of OH_{ad} by reaction with hydrogen is not possible, because this would cause further catalyst reduction beyond steady-state conditions. In the presence of H_2 (2 kPa H_2), adsorption of CO leads to more formates on the surface, which can be explained by the reaction of H_2 and bidentate carbonates. Bidentate (1291 cm^{-1}) and monodentate (1420 cm^{-1}) carbonates were formed by reaction of CO with the surface in all cases (see Section 3.3). During CO adsorption under all conditions, with further increasing H_2 partial pressure, the intensity of the formate-related peaks increases and the signal shifts to lower wavenumbers, from 2845 to 2837 cm^{-1}. This shift is likely related to formate–formate interactions at increasing formate coverages. In addition, at a H_2 partial pressure of 50 kPa, a new peak with maxima at 2936–2961 cm^{-1} emerges, which is attributed to bridged formates (Table 3 or [24,30]) and has the greatest intensity at the highest H_2 concentration.

Similar trends—in particular, a similar development of adsorbed formates—were observed during the WGS reaction on Au/CeO_2 at 180 °C under comparable conditions in idealized reformate with increasing H_2 content. DRIFT spectra recorded under steady-state conditions after 1000 min of reaction (Fig. 9, right panel) show that up to a H_2 partial pressure of 50 kPa H_2, bidentate formates with a peak at 2833 cm^{-1} dominate the spectrum, and their intensity increases with higher H_2 partial pressure. A drastic change in the C–H region signal was observed at the highest H_2 partial pressure of 97 kPa. Under these

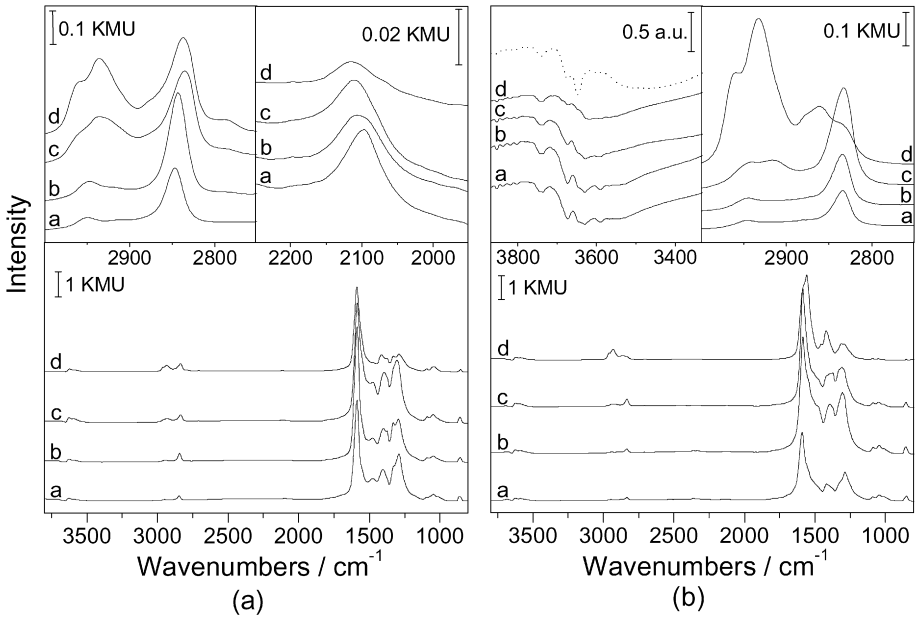

Fig. 9. Left panel: selected spectra from a sequence of DRIFT spectra recorded during adsorption of CO (0.5 kPa CO) from CO/N_2 atmospheres with increasing H_2 partial pressures on a 2.7 wt% Au/CeO_2 catalyst at 180 °C (steady-state conditions): (a) 0 kPa, (b) 2 kPa, (c) 50 kPa, (d) 97 kPa H_2, balance N_2. Bottom panel: full spectrum; top left panel: detail spectra of the C–H stretch region; top right panel: detail spectra of the CO_{ad} region). Right panel: selected spectra from a sequence of DRIFT spectra recorded during the WGS reaction at 180 °C on a 2.7 wt% Au/CeO_2 catalyst in idealized reformate (1 kPa CO, 2 kPa H_2O, balance N_2) with increasing H_2 partial pressures (steady-state conditions): (a) 0 kPa, (b) 2 kPa, (c) 50 kPa, (d) 97 kPa H_2, balance N_2. Bottom panel: full spectra; top left panel: detail spectra of the O–H stretch region; top right panel: detail spectra of the C–H stretch region.

conditions, the intensity of the bidentate formate at 2833 cm^{-1} is strongly reduced and the peak shifts to 2859 cm^{-1}. Instead, the peaks at 2933 and 2961 cm^{-1}, indicative of bridged formates, dominate this region. Together with the shift in the C–H vibration of the bidentate formate, the corresponding OCO peak at 1590 cm^{-1} shifts to 1562 cm^{-1}. Interestingly, the intensity of the O–H signals (Fig. 9, right panel) decreases with increasing H_2 partial pressure. Most likely, this change in O–H intensity results from a reaction of the OH groups with hydrogen and its removal as H_2O ($H_2 \rightarrow 2H_{ad}$, $H_{ad} + OH_{ad} \rightarrow H_2O_{ad}$, $H_2O_{ad} \rightarrow H_2O_g$). This explanation is supported by the significantly higher H_2O reaction order in the H_2-rich realistic reformate than in the H_2-free idealized reformate. For lower H_2O partial pressures, the removal of OH groups by reaction with hydrogen overcompensates for the build-up of OH groups by reaction of the surface with H_2O, whereas at higher H_2O pressures, this effect is less important. This explains the higher reaction order for H_2O observed in realistic reformate. Competitive adsorption between H_2O and hydrogen on the same adsorption sites, as proposed by Sakurai et al. [8], is considered less likely.

Overall, our results support the assumptions that CO_{ad} and H_{ad} are coadsorbed on the Au particles and that hydrogen removes surface OH groups through reaction to H_2O. This explains the higher reaction orders for CO and H_2O in realistic reformate compared with idealized reformate [5].

3.6. Reverse WGS reaction

In this section, we focus on the question of how the presence of CO_2 and H_2 can affect the reaction (particularly the adlayer by direct reaction) through the reverse WGS (RWGS) reaction and to what extent. The reaction and the build-up of the resulting adlayer were studied on a 4.5 wt% Au/CeO_2 catalyst in the absence of CO and H_2O (1 kPa CO_2, 1 kPa H_2, balance N_2 at 180 °C), with the adsorbate intensities determined by time-resolved DRIFTS measurements. The resulting reaction rates of 6.5×10^{-6} mol g_{Au}^{-1} s^{-1} (90.3 mg of catalyst) after 17 min and 4.4×10^{-6} mol g_{Au}^{-1} s^{-1} after 120 min (32% deactivation over 100 min) are significantly lower than those of the WGS reaction.

A sequence of selected DRIFT spectra recorded during the reaction is shown in Fig. 10. Also under these conditions, formates are formed (cf. [28,31–34] for Pt/CeO_2), with characteristic peaks at 2945 and 2845 cm^{-1} in the beginning of the reaction. The latter peak appears at higher frequencies compared with the bidentate formate signal obtained during the forward shift reaction in idealized reformate (2833 cm^{-1}), but resembles that observed during CO adsorption from CO/N_2 mixtures on Au/CeO_2 (see Section 3.5). After 60 min of reaction, the peak at 2845 cm^{-1} starts shifting to 2863 cm^{-1}, and the correlated OCO peak at 1585 cm^{-1} moves to lower wavenumbers (1562 cm^{-1}). At the same time, the peak at 2945 cm^{-1} increases significantly and splits into two new bands at 2963 and 2934 cm^{-1}. The less reactive formates with characteristic peaks at 2963, 2934, 2863, and 1562 cm^{-1} (see Section 3.3) dominate the spectrum after 1000 min of reaction time. Furthermore, we see monodentate and bidentate carbonates in the OCO region, identical to the WGS reaction in the various gas mixtures presented so far. Again, monodentate carbonates increase and bidentate carbonates decrease during the reaction. The bridged OH groups at 3647 cm^{-1} that are present at the beginning of the reaction disappear completely within 5 min of reaction.

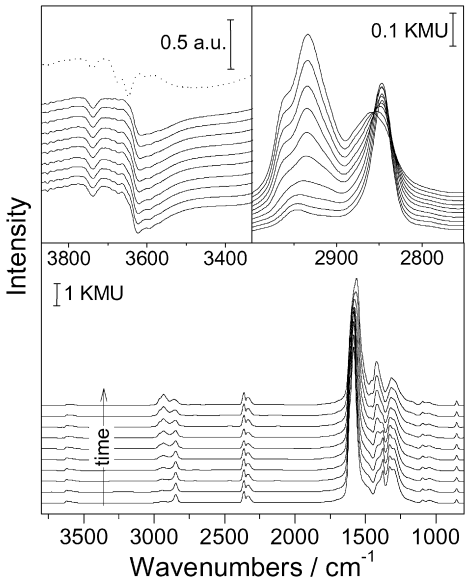

Fig. 10. Selected spectra from a sequence of DRIFT spectra recorded during the RWGS reaction on an Au/CeO_2 catalyst at 180 °C in 1 kPa CO_2, 1 kPa H_2, rest N_2 (gas flow 80 Nml min^{-1}, 40–50 mg 4.5 wt% Au/CeO_2 catalyst, reaction times: 15, 30, 60, 120, 240, 360, 480, 600, 780, and 1020 min). Bottom panel: full spectra; top left panel: detail spectra of the O–H stretch region; top right panel: detail spectra of the C–H stretch region.

This finding correlates with the foregoing interpretation that hydrogen removes the OH groups through reaction to H_2O (see Section 3.5). Because the reactive atmosphere contains 99 kPa H_2 and no H_2O, no OH groups are produced, resulting in the removal of these species (see Section 3.5).

Overall, the development of the adsorbed formate species (in particular, the change from bidentate to bridged formates and the shift of the bidentate formates to higher wavenumbers) resembles that observed during the WGS reaction in $H_2 + CO_2$-rich and (CO_2-free) H_2-rich atmospheres. On the other hand, the spectra differ significantly from those obtained during reaction in idealized reformate; that is, the less reactive formates (2963, 2934, 2863, and 1562 cm^{-1}; see Section 3.3) are built up in the former case only. This supports the assumption that the reduction of the support by H_2 and subsequent modification of the adsorption sites are essential for the build-up of these less active formate species. Tabakova et al. [41] also studied the RWGS reaction on an Au/CeO_2 catalyst and found no build-up of additional formates. Most likely, this is explained by their experimental procedure, which involved preadsorbing hydrogen before adding CO_2 for 15 min at different temperatures (from room temperature up to 200 °C) rather than exposing the catalyst to a reaction mixture. In addition, Goguet et al., who studied the RWGS reaction on a Pt/CeO_2 catalyst with a H_2 concentration of 4% by DRIFTS, observed no additional formate formation [31,43]. This agrees well with our observation that H_2-induced catalyst reduction occurs at very high H_2 partial pressures.

Overall, our findings confirmed (see Sections 3.2 and 3.3) reduction of the support under high H_2 partial pressures, resulting in generation of new adsorption sites and, consequently, buildup of the less reactive formate species characterized by vibrational bands at 2861 and 2969 cm^{-1}.

4. Discussion

The data presented herein and in previous studies lead to the following conclusions on the reaction mechanism and on the deactivation of Au/CeO_2 catalysts in the low-temperature WGS reaction:

1. Reaction in idealized reformates leads to the formation of surface formates and surface carbonates, the latter likely resulting from reaction with CO_2 produced during the WGS reaction. Surface formates have been identified as reaction intermediates on this catalyst [5]. Monodentate carbonates act as reaction-inhibiting spectator species, reducing the number of sites available for accommodating surface formates or for CO adsorption. The area of the capture zone for CO is reduced [5]. The data are compatible with our recent mechanistic proposal, which involves (i) formate formation and decomposition on active sites, most likely at the interface between Au nanoparticles and support, (ii) reverse spillover of these formates on the support and vice versa, and (iii) adsorption of CO directly on Au nanoparticles or on the support, followed by reverse spillover on the Au nanoparticles (CO adsorption with a capture zone) [5].
2. In the presence of CO_2 in the gas mixture, both monodentate carbonate formation and deactivation increase with increasing CO_2 content. This supports the assumption that in idealized reformate, product CO_2 is involved in carbonate formation. Furthermore, the lower deactivation during the WGS reaction at higher reaction temperatures [20,21] can easily be understood by the increasing thermal decomposition and hence lower steady-state coverage of reaction-inhibiting carbonate species.
3. The presence of H_2 has little effect on the deactivation behavior, but significantly reduces the initial activity. This can be explained by an increasing back-reaction (RWGS reaction), as shown by the IR data. In H_2-rich idealized reformate, more formates (2833 cm^{-1}) are seen within the first 15 min of the reaction compared with the amount in idealized reformate, because these formates can be built up via both the WGS and the RWGS. During further reaction, less reactive bidentate and, in particular, bridged formate species are formed, at the expense of the 2833 cm^{-1} bidentate formate species. This finding is tentatively explained by the increasing reduction of the support surface. Because deactivation is not affected by these changes, poisoning by the additional (less reactive) formates can be excluded.
4. Bidentate carbonates are formed at the beginning of the reaction in all reaction atmospheres. In contrast to the monodentate carbonates, they decrease in amount during the reaction, and thus they cannot be responsible for long-term deactivation. Their temporal evolution resembles that of the reactive bidentate formates (see Fig. 4 and Table 4). Therefore, these species may be in a dynamic equilibrium with the reactive bidentate formate species. This is also sup-

ported by the observation that their absolute intensity is smaller under steady-state conditions in H_2-rich idealized reformate than in idealized reformate, similar to the absolute intensities of bidentate formates. From the results of the transient experiment in Section 3.3, it is obvious that bidentate and, in particular, bridged formates can be produced by reaction of bidentate carbonate with H_2.

5. The high reaction orders of 1.0 for CO and H_2O in the WGS reaction in realistic reformate reveal a significantly greater influence of these two components on the reaction rate compared with that seen in idealized reformate [5]. The higher CO reaction order is related to the coadsorption of CO and hydrogen on gold particles. The higher H_2O reaction order is explained by the decrease in OH groups on the support by reaction with hydrogen. At low H_2O partial pressures, this OH removal overcompensates for their build-up from the H_2O present in the gas phase. In turn, the OH group concentration determines the rate of formate formation. For CO_2 and H_2, we obtained reaction orders of -0.5 and -0.7, respectively, nearly identical to the values obtained in idealized reaction reformate [5]. Apparently, the increased presence of adsorbed hydrogen or CO_2 does not cause significant modification of the reaction characteristics, in contrast to their effect on the reaction rate and the formation and stability of reaction side products.
6. The IR measurements during the WGS reaction in various realistic reformates reveal the same intermediate and side products as in idealized reformate, supporting the previously stated conclusion that the reaction characteristics are not significantly altered by the presence of CO_2 or H_2. Most importantly, monodentate carbonates, which are present with significantly higher concentrations in CO_2-containing atmosphere, increase deactivation by blocking adsorption sites on the ceria support and possibly (to a small extent of their total coverage) active sites as well. Furthermore, similar to idealized reformate, higher H_2 concentrations cause a faster build-up of the less reactive bidentate and bridged formate species.
7. For the RWGS reaction, the temporal evolution of all formate species—the reactive bidentate formates as well as of the less reactive formates—is similar to their temporal evolution during the WGS reaction in H_2-rich atmosphere. This further supports (see point 3) that the change in adsorbed formate species is determined by the ongoing reduction of the ceria support in both cases.

Finally, for application in PEFC feed gas processing, for CO removal from realistic reformate, these results indicate that both the initial activity and long-term activity are significantly lower in realistic reformate than in idealized reformate. Therefore, studies on the WGS performance of Au/CeO_2 catalysts performed in idealized reformate, as it is commonly done, will result in data for the initial activity and the long-term stability that are much better than what would be expected for operation in realistic reformate. As shown earlier, high H_2 concentrations lead to a significant drop in the initial activity, whereas CO_2 affects deactivation behavior through an increasing tendency for carbonate formation. The latter tendency can be decreased by H_2 in the feed gas, which converts (reaction-inhibiting) carbonates into (reactive) formates. However, at the high CO_2 concentrations present in realistic reformate, this latter reaction is not fast enough and is overcompensated for by the rapid carbonate formation due to reaction with CO_2.

These counteracting trends explain, in a straightforward way, the significant discrepancies in previous data on the WGS performance of the Au/CeO_2 catalyst, with significant variations in the composition of the reaction gas mixtures. In addition, effects resulting from variation in catalyst synthesis and conditioning and the specific reaction conditions (particularly the reaction temperature) may further affect the reactivity. Higher reaction temperatures are expected to improve the long-term stability due to more rapid carbonate decomposition. At excessively high temperatures, we would expect this effect to be (over)compensated for by Au nanoparticle sintering.

Consequently, further optimization of supported Au catalysts for PEFC feed gas processing will require distinct improvements in the sensitivity toward carbonate formation (deactivation), the sensitivity toward high H_2 partial pressure (initial activity), and the stability of the catalyst toward sintering of Au nanoparticles, which should be sufficient so that this process can be excluded at temperatures sufficient to keep the steady-state carbonate coverage at tolerable levels.

5. Conclusion

We have shown, by combined kinetic and in situ IR spectroscopic measurements in different reaction atmospheres, that both the activity and stability of the Au/CeO_2 catalyst in the WGS reaction at 180 °C are affected by the composition of the reaction atmosphere and the presence of CO_2 and H_2. Kinetic measurements have revealed that H_2 significantly reduces the initial reaction rate but has little effect on deactivation. In contrast, the effect of CO_2 on the initial reaction rate is small but results in a much more pronounced deactivation. This latter effect increases with increasing CO_2 content and is mainly responsible for the enhanced deactivation in realistic reformate.

In situ DRIFTS measurements resolve a number of different adsorbed reactants, reaction intermediates, side products, and products, including OH groups, CO_{ad} and CO_2, bidentate and bridged formats, and monodentate and bidentate carbonates. The exact composition of the adlayer and its exact chemical state are highly dependent on the reaction atmosphere and on the oxidation state of the CeO_2 support surface. In all reaction atmospheres, the decreased reaction rate during the reaction occurs along with an increase in monodentate carbonate. Together with other results, this implies that this species, which is also thermally most stable, acts as rate-inhibiting spectator species by blocking ceria surface sites for adsorbed formate accommodation and/or decreasing the area available for CO adsorption on the support and subsequent inverse spillover to the Au nanoparticles (capture zone), and also possibly blocking active sites as well. The data are consistent with an assignment of bidentate formates as reaction intermediates, indicating that the reaction pathway that we recently proposed for the WGS

reaction in idealized reformate [5], via formation and decomposition of bidentate formats, with formate decomposition as the rate-limiting step, is dominant in realistic reformate as well.

The significant CO content in realistic reformate further enhances deactivation, most likely by monodentate carbonate formation through continuing formation of product CO_2. For practical applications, higher operating temperatures are beneficial due to the increased decomposition of reaction-inhibiting carbonate species, as long as the temperature is low enough to exclude significant sintering of the Au nanoparticles.

Acknowledgments

Financial support was provided by the Landesstiftung Baden-Württemberg and the Deutsche Forschungsgemeinschaft (Be 1201/9-4).

Supplementary material

The online version of this article contains additional supplementary material.

Please visit DOI:10.1016/j.jcat.2006.11.012.

References

[1] R. Kumar, S. Ahmed, in: O. Savadogo, P.R. Roberge, T.N. Veziroglu (Eds.), Fuels Processing for Transportation Fuel Cell Systems, 32767 BC, Les Éditions de l'École Polytechnique de Montréal, Montréal, Québec, Canada, 1995, pp. 224–238.
[2] D.L. Trimm, Z.I. Önsan, Catal. Rev. 43 (2001) 31.
[3] S. Gottesfeld, T.A. Zawodzinski, in: R.C. Alkire, H. Gerischer, D.M. Kolb, C.W. Tobias (Eds.), Advances in Electrochemical Science and Engineering, vol. 5, Wiley–VCH, Weinheim, 1997.
[4] K. Kochloefl, in: G. Ertl, H. Knözinger, J. Weitkamp (Eds.), Handbook of Heterogeneous Catalysis, vol. 2, Wiley–VCH, Weinheim, 1997.
[5] R. Leppelt, B. Schumacher, V. Plzak, M. Kinne, R.J. Behm, J. Catal. 244 (2006) 137.
[6] C.H. Kim, L.T. Thompson, J. Catal. 230 (2005) 66.
[7] Q. Fu, W. Deng, H. Saltsburg, M. Flytzani-Stephanopoulos, Appl. Catal. B 56 (2005) 57.
[8] H. Sakurai, T. Akita, S. Tsubota, M. Kiuchi, M. Haruta, Appl. Catal. A 291 (2005) 179.
[9] J.M. Zalc, V. Sokolovskii, D.G. Loeffler, J. Catal. 206 (2002) 169.
[10] X. Wang, R.J. Gorte, Appl. Catal. A 224 (2002) 209.
[11] A. Luengnaruemitchai, S. Osuwan, E. Gulari, Catal. Commun. 4 (2003) 215.
[12] X. Liu, W. Reuttinger, X. Xu, R. Farrouto, Appl. Catal. B 56 (2005) 69.
[13] D. Andreeva, V. Idakiev, T. Tabakova, L. Ilieva, P. Falaras, A. Bourlinos, A. Travlos, Catal. Today 72 (2002) 51.
[14] B. Schumacher, V. Plzak, M. Kinne, R.J. Behm, Catal. Lett. 89 (2003) 109.
[15] V. Plzak, J. Garche, R.J. Behm, Eur. Fuel Cell News 10 (2003) 16.
[16] M.J. Kahlich, H.A. Gasteiger, R.J. Behm, J. Catal. 171 (1997) 93.
[17] P.B. Weisz, Chem. Eng. Prog. Symp. Ser. 55 (1992) 29.
[18] M.M. Schubert, M.J. Kahlich, H.A. Gasteiger, R.J. Behm, J. Power Sources 84 (1999) 175.
[19] I.M. Hamadeh, P.R. Griffiths, Appl. Spectrosc. 41 (1987) 682.
[20] Q. Fu, S. Kudriavtseva, H. Saltsburg, M. Flytzani-Stephanopoulos, Chem. Eng. J. 93 (2003) 41.
[21] Q. Fu, A. Weber, M. Flytzani-Stephanopoulos, Catal. Lett. 77 (2001) 87.
[22] Q. Fu, H. Saltsburg, M. Flytzani-Stephanopoulos, Science 301 (2003) 935.
[23] C. Li, Y. Sakata, T. Arai, K. Domen, K. Maruya, T. Onishi, J. Chem. Soc. Faraday Trans. 85 (1989) 1451.
[24] T. Shido, Y. Iwasawa, J. Catal. 136 (1992) 493.
[25] T. Shido, Y. Iwasawa, J. Catal. 141 (1993) 71.
[26] C. Li, Y. Sakata, T. Arai, K. Domen, K. Maruya, T. Onishi, J. Chem. Soc. Faraday Trans. 85 (1989) 929.
[27] F. Bozon-Verduraz, A. Bensalem, J. Chem. Soc. Faraday Trans. 90 (1994) 653.
[28] C. Binet, M. Daturi, J.-C. Lavalley, Catal. Today 50 (1999) 207.
[29] J.-D. Grunwaldt, A. Baiker, J. Phys. Chem. B 103 (1999) 1002.
[30] G. Jacobs, L. Williams, U. Graham, G.A. Thomas, D.E. Sparks, B.H. Davis, Appl. Catal. 252 (2003) 107.
[31] A. Goguet, F.C. Meunier, D. Tibiletti, J.P. Breen, R. Burch, J. Phys. Chem. B 108 (2004) 20240.
[32] F.C. Meunier, D. Tibiletti, A. Goguet, D. Reid, R. Burch, Appl. Catal. A 289 (2005) 104.
[33] D. Tibiletti, A. Goguet, F.C. Meunier, J.P. Breen, R. Burch, Chem. Commun. (2004) 1636.
[34] D. Tibiletti, A. Goguet, D. Reid, F.C. Meunier, R. Burch, Catal. Today 113 (2006) 94.
[35] S. Hilaire, X. Wang, T. Luo, R.J. Gorte, J. Wagner, Appl. Catal. A 215 (2001) 271.
[36] N.A. Koryabkina, A.A. Phatak, W.F. Ruettinger, R.J. Farrauto, F.H. Ribeiro, J. Catal. 217 (2003) 233.
[37] S. Hilaire, X. Wang, T. Luo, R.J. Gorte, J. Wagner, Appl. Catal. A 258 (2004) 271.
[38] T. Bunluesin, R.J. Gorte, G.W. Graham, Appl. Catal. B 15 (1998) 107.
[39] E. Bus, J.T. Miller, J.A. van Bokhoven, J. Phys. Chem. B 109 (2005) 14581.
[40] J. Guzman, S. Carrettin, A. Corma, J. Am. Chem. Soc. 127 (2005) 3286.
[41] T. Tabakova, F. Boccuzzi, M. Manzoli, D. Andreeva, Appl. Catal. A 252 (2003) 385.
[42] M. Daturi, E. Finocchio, C. Binet, J.C. Lavalley, F. Fally, V. Perrichon, J. Phys. Chem. B 103 (1999) 4884.
[43] A. Goguet, F. Meunier, J.P. Breen, R. Burch, M.I. Petch, A. Faur Ghenciu, J. Catal. 226 (2004) 382.
[44] E. Finocchio, M. Daturi, C. Binet, J.C. Lavalley, G. Blanchard, Catal. Today 52 (1999) 53.